SIMPLIFIED APPROACH FOR ESTIMATING THE ENVELOPE RESPONSE OF UNBONDED-POSTTENSIONED MASONRY SHEAR WALLS

Kalliontzis, Dimitrios[1]; Schultz, Arturo[2] and Sri Sritharan[3]

ABSTRACT

There is a growing interest in understanding the in-plane behavior of unbonded-posttensioned walls to develop wall systems that can re-center with small residual deformations and little damage when subjected to horizontal seismic loads. However, conventional analysis methods cannot reproduce the response characteristics of unbonded-posttensioned masonry walls accurately, as a) there is strain incompatibility between masonry and the unbonded bars; and b) these walls respond primarily by rocking, which concentrates the wall deformations at the base. Due to the walls' rocking response, the neutral axis depth at the base of the wall tends to decrease with increasing posttensioning force and wall lateral displacement, while the wall toe region experiences confinement from lateral friction at the wall-to-foundation interface. This paper presents an approach to address the response characteristics pertaining to these wall systems by using an analysis method that enables the walls to respond in a mixed mechanism of rocking, flexure, and shear responses. The analysis method is shown to improve correlation to experimental results compared to analyses that assume only a rocking response.

KEYWORDS: *rocking, masonry, unbonded-posttensioned, self-centering, shear wall*

INTRODUCTION

There is evidence that rocking as a mechanism for seismic resistance has been utilized from ancient times. For example, the segmental construction of temples in ancient Greece enabled these structures to rock by allowing gap openings between the columns, the base, and the entablature. However, the seismic performance of rocking structures has not been investigated systematically until recently. The earliest fundamental treatment is attributed to Housner [1], who showed analytically that allowing structural members to rock may reduce their seismic-force demands.

[1]Ph. D. Student, Department of Civil, Environmental, and Geo-Engineering, University of Minnesota, Twin Cities, Minneapolis, MN, United States, 55455, kalli072@umn.edu
[2]Professor, Department of Civil, Environmental, and Geo-Engineering, University of Minnesota, Twin Cities, Minneapolis, MN, United States, 55455, schul088@umn.edu
[3]Wilkinson Chair Professor in Engineering, Iowa State University, Ames, IA, 50011-3232, sri@iastate.edu

Housner's analytical findings on the seismic response of rocking structures encouraged their application in contemporary structural systems. The use of rocking to create re-centering walls for modern building construction was realized during the Precast Seismic Structural Systems (PRESSS) program by Priestley et al., and Schultz et al. [2, 3]. These researchers tested rocking precast-concrete walls with unbonded-posttensioning using quasi-static test schemes. They observed the walls to experience minimal damage, which was concentrated at the wall bottom toes, and re-center with negligible residual displacements. Following the experimental observations, several rocking precast-concrete wall systems have been developed (e.g., the Precast Walls with End Columns (PreWEC) system by Sritharan et al. [4]) and other research studies investigated the behavior of rocking precast-concrete structures using means of dynamic excitation [5-8].

With the research findings indicating significant advantages resulting from the rocking mechanism, this mechanism has been used to design masonry walls with unbonded-posttensioning [9-13]. Experiments indicated that rocking masonry walls experience reduced damage and enhanced re-centering capacity. Laursen and Ingham [12] observed experimentally that these walls respond primarily by rocking, but also that flexure and shear can be noticeable in their responses. More recently, Kalliontzis and Schultz [14] showed that rocking masonry walls experience a confinement effect due to lateral friction at the wall-to-foundation interface, and [15] confirmed using finite element analyses that the responses of rocking masonry walls include rocking, flexure, and shear displacement components.

This paper introduces an analysis method to estimate the envelope responses of rocking masonry walls by allowing three response mechanisms: rocking, flexure, and shear. The method also accounts for the aforementioned confinement effect at the wall-to-foundation interface.

ANALYSIS METHOD

The analysis method presented here employs iterative sectional analysis at the wall-to-foundation interface and is based on the following assumptions:

1. A joint is assumed to open at the wall-to-foundation interface.
2. The masonry wall is subjected to in-plane deformations and will respond in three mechanisms: rocking, flexure, and shear, as is demonstrated in Figure 1. Accordingly, wall deformations due to rocking occur below the compression zone height (designated as Z_c), while the opposite wall toe lifts off at the base. Due to the toe uplift, flexure and shear deformations occur within the compression zone and the part of the wall above Z_c, as shown. Being small components of the overall wall responses, flexure and shear are modelled as linear mechanisms. Nonlinear analysis is employed for the rocking mechanism, which dominates the wall response.
3. Rocking, flexure, and shear mechanisms are treated as springs in series, such that they carry the same amount of force, but their deflections are additive:
    - The total in-plane displacement Δ_{total} at the top of the wall equals the sum of the displacements due to rocking $\Delta_{rocking}$, flexure $\Delta_{flexure}$, and shear Δ_{shear}.

- Assuming a wall in-plane force F_{total} at Δ_{total}, the corresponding force to each mechanism is F_{total} (i.e., $F_{total} = F_{rocking} = F_{flexure} = F_{shear}$).

4. The friction resistance at the wall-to-foundation interface prevents the wall from sliding relative to the foundation.

5. The lateral friction at the wall-to-foundation interface produces lateral confinement on masonry, which increases the stress and strain capacities of masonry in the compression zone [14].
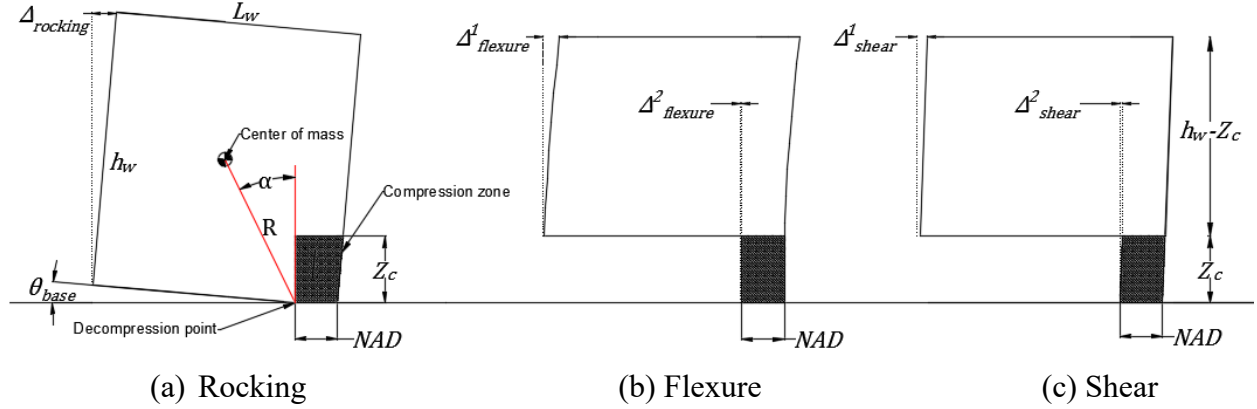

(a) Rocking   (b) Flexure   (c) Shear

Figure 1: Demonstration of the three response mechanisms accounted in the analysis method

The analysis method is implemented in MATLAB using the routine outlined below, which estimates the envelope response of a rocking masonry wall. It includes estimation of the flexure and shear responses and a subroutine that computes the nonlinear rocking response. A thorough description of this subroutine can be found in [14] and only a brief summary is included here.

Routine to estimate total wall response

Step 1: Define an increment for the total wall displacement Δ_{total} $d\Delta_{total}$, such that:

$$\Delta_{total} = d\Delta_{total} + \Delta_{total,previous} \tag{1}$$

where $\Delta_{total,previous}$ denotes the total wall displacement at the end of the previous step.

Step 2: Select an estimate for the rotation at the wall base θ_{base}, which should satisfy the condition $\theta_{base,previous} < \theta_{base}$, where $\theta_{base,previous}$ is the wall base rotation from the previous step. Next, use the subroutine to estimate $F_{rocking}$.

Step 3: Compute the stiffness of the flexure $K_{flexure}$ and shear K_{shear} mechanisms, and the secant stiffness of the rocking mechanism $K_{rocking,secant}$ as follows:

$$\Delta_{flexure} = \Delta^1{}_{flexure} + \Delta^2{}_{flexure} = \frac{F_{total}(h_w - Z_c)^3}{3E_m I_n} + \frac{F_{total} Z_c{}^3}{3E_m I_{Z_c}} \geq \frac{F_{total} h_w{}^3}{3E_m I_n} \tag{2}$$

$$\Delta_{shear} = \Delta^1{}_{shear} + \Delta^2{}_{shear} = \frac{1.2 F_{total}}{G_m l_w t_w}(h_w - Z_c) + \frac{1.2 F_{total}}{G_m Z_c t_w} Z_c \geq \frac{1.2 F_{total} h_w}{G_m l_w t_w} \tag{3}$$

where I_n denotes the net moment of inertia of the wall; I_{z_c} denotes the net moment of inertia corresponding to the compression zone; E_m is the modulus of elasticity of masonry, which is computed per MSJC [16] as $E_m = 900f'_m$; G_m is the shear modulus of masonry, which is estimated as $G_m = 0.4E_m$; l_w, h_w and, t_w are the wall length, height, and thickness, respectively. Same as in Kalliontzis and Schultz [14], it is assumed that $Z_c = 1.5NAD \leq h_w$, where NAD denotes the neutral axis depth at the wall-to-foundation interface (see Figure 1), which is estimated in the subroutine. Accordingly:

$$K_{flexure} = \frac{\Delta_{flexure}}{F_{wall}} = \frac{\frac{3E_m I_n}{(h_w - Z_c)^3}}{1 + \left(\frac{Z_c}{h_w - Z_c}\right)^3 \left(\frac{l_w}{NAD}\right)^3} \leq \frac{3E_m I_n}{h_w{}^3} \tag{4}$$

$$K_{shear} = \frac{\Delta_{shear}}{F_{wall}} = \frac{\frac{E_m l_w t_w}{3(h_w - Z_c)}}{1 + \frac{l_w}{h_w - Z_c}} \leq \frac{E_m l_w t_w}{3h_w} \tag{5}$$

$$K_{rocking,secant} = \frac{F_{rocking} - F_{rocking,previous}}{(\theta_{base} - \theta_{base,previous})h_w} \tag{6}$$

where estimation of $K_{flexure}$ and K_{shear} uses the estimate for NAD.

Step 4: Based on the estimated stiffness of each mechanism, compute the corresponding displacement contributions as follows:

$$\Delta_{flexure} = \Delta_{flexure,previous} + \frac{d\Delta_{total}}{1 + \frac{K_{flexure}}{K_{shear}} + \frac{K_{flexure}}{K_{rocking,secant}}} \tag{7}$$

$$\Delta_{shear} = \Delta_{shear,previous} + \frac{d\Delta_{total}}{1 + \frac{K_{shear}}{K_{flexure}} + \frac{K_{shear}}{K_{rocking,secant}}} \tag{8}$$

$$\Delta_{rocking} = \left[\theta_{base,previous}h_w + \left(d\Delta_{total} - d\Delta_{flexure} - d\Delta_{shear}\right)\right] \tag{9}$$

with

$$\Delta_{total} = \Delta_{flexure} + \Delta_{shear} + \Delta_{rocking} \tag{10}$$

Step 5: If the computed θ_{base} per Eq. 9 (i.e., $\theta_{base} = \Delta_{rocking}/h_w$) does not meet the limitations defined in **Step 2**, return to **Step 2** to update θ_{base}. If there is convergence on θ_{base}, repeat the routine for Δ_{total} of the next increment.

Subroutine to compute wall response due to rocking
Step 1: Determine an initial estimate of NAD corresponding to θ_{base}.

Step 2: Compute the total compressive masonry force C_m. C_m can be estimated using Eq. 11:

$$C_m = t_w \int_0^{NAD} f_{cm}[\varepsilon_m(x)]\, dx \tag{11}$$

where f_{cm} is the confined compressive masonry stress computed as a function of the masonry strain $\varepsilon_m(x)$. f_{cm} is estimated using the confined masonry stress-strain curves presented by Priestley and Elder [17]. The peak masonry stress, f'_{cm}, which defines the maximum value in these curves, is computed by accounting for the confinement due to lateral friction at the wall-to-foundation interface, as described in [14]. Same as in [14], $\varepsilon_m(x)$ is estimated as follows:

$$\varepsilon_m(x) = \frac{x}{NAD}\left(\theta_{base}\frac{NAD}{z_c} + \varepsilon_o\right) \tag{12}$$

with ε_o being the initial, uniformly distributed, compressive masonry strain due to the initial post-tensioning force and wall self-weight; and x denotes the distance between the decompression point and a point within the NAD.

Step 3: Compute the tension force, T, using Eq. 13:

$$T = \Sigma(f_{PT}A_{PT}) + W \tag{13}$$

where W is the wall self-weight and $\Sigma(f_{PT}A_{PT})$ represents the total posttensioning force, which accounts for the posttensioned steel bar elongations due to $\Delta_{rocking}$. No increase in posttensioning force is assumed due to flexure and shear, as it is small compared to the increase due to rocking.

Step 4: If $C_m \neq T$, go back to **Step 1** and revise the value for NAD. If C_m and T are sufficiently close, continue to **Step 5**.

Step 5: Compute the base moment of the wall for the current analysis step using Eq. 14:

$$M_{rocking} = \Sigma f_{PT}A_{PT}D_{bar} + WRsin(\alpha - \theta_{base}) + t_w \int_0^{NAD} f_{cm}[\varepsilon_m(x)]x \, dx \tag{14}$$

where α is shown in **Figure 1** and can be defined as:

$$\alpha = tan^{-1}\left[\frac{\frac{l_w}{2}-NAD}{\frac{h_w}{2}}\right] \tag{15}$$

D_{bar} denotes the moment-arm of the posttensioned bar force; and R is the distance between the decompression point and the center of mass of the wall.

Step 6: Assuming a lateral concentrated force at h_w, the wall lateral-force resistance is estimated as:

$$F_{rocking} = \frac{M_{rocking}}{h_w} \tag{16}$$

VERIFICATION

Two quasi-static, reverse-cyclic, tests of fully-grouted concrete masonry walls with unbonded-posttensioning tested by Laursen and Ingham [9] are used to verify the proposed analysis method.

Properties of the test walls are presented in Table 1. Both walls were posttensioned using two unbonded threaded bars, which were symmetrically distributed along the wall length with spacing of S_{PT}, as indicated in the table. The bars had unbonded length of 3.5 m, yield strength of 970 MPa, ultimate strength of 1,160 MPa, and modulus of elasticity of 190 GPa. Compressive strengths, f'_m, of the concrete masonry assemblies were estimated using prism tests.

Based on the experimental observations, the two wall responses were dominated by a rocking response with their strength degradation being attributed to crushing of masonry at the wall compression toes and yielding of the unbonded-posttensioned (UPT) steel bars.

Table 1: Properties of the two masonry walls with unbonded-posttensioning tested by Laursen and Ingham [9]

Wall	$*^{(1)}l_w$, m	$*^{(2)}h_w/l_w$, m	$*^{(3)}t_w$, m	# UPT bars	$*^{(4)}f'_m$, MPa	$*^{(5)}F_{PTi}$, kN	$*^{(6)}S_{PT}$, m	$*^{(7)}d_{bl}$, mm
Wall 1	3.0	0.93	0.14	2	20.6	622	0.8	23
Wall 2	1.8	1.55	0.14	2	20.5	445	0.8	23

$*^{(1)}$ Wall length
$*^{(2)}$ Wall height/length
$*^{(3)}$ Wall thickness
$*^{(4)}$ Experimentally estimated concrete masonry strength
$*^{(5)}$ Total initial posttensioning force
$*^{(6)}$ Horizontal spacing between the unbonded-posttensioning steel bars.
$*^{(7)}$ Diameter of the unbonded-posttensioning steel bars.

Figure 2 presents the force-displacement responses as produced by the analysis method for the two walls and compares them with the force-displacement envelopes established from the experimental reverse-cyclic responses. The comparisons show that the analysis method adequately captures the response envelope of Wall 2 and up to peak response for Wall 1. Differences between analysis and the envelopes are in part because the monotonic analyses were unable to accurately reproduce the characteristics of reverse-cyclic wall responses. These include degradation of masonry and the reduction in initial posttensioning force upon re-centering of the walls, which have been observed experimentally. For example, based on experimental measurements for Walls 1 and 2, their initial post-tensioning forces were reduced by about 75% and 25%, respectively, at the end of their tests, indicating a significant effect specifically in the experimental response of Wall 1. Such effect was not included in the monotonic analyses. As shown by Kalliontzis and Schultz [15], accounting for the reverse-cyclic displacements of the walls in the analyses significantly improves correlation with the experimental force-displacement envelopes.
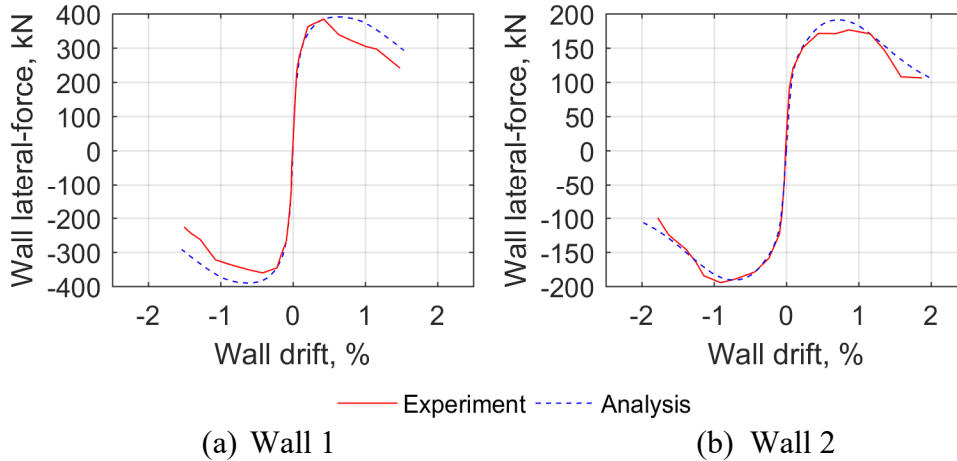
(a) Wall 1   (b) Wall 2

Figure 2: Wall lateral-force resistance vs. wall top in-plane drift

Table 2 presents the wall peak strengths as estimated by the analysis method and from the experiments. It also includes wall peak strengths computed by assuming that the walls would respond only by rocking [14]. The comparisons in Table 2 indicate that the analysis method introduced herein agrees well with the experimentally measured wall peak strengths.

Table 2: Wall peak strengths by the analysis method, analysis that includes only the rocking mechanism, and experimental measurements.

Wall	Peak wall strength, kN		
	Analysis	Analysis, Only Rocking	Experiment
Wall 1	391	392	384
Wall 2	191	191	195

Figure 3 presents the total posttensioning forces with respect to the wall top in-plane drifts as estimated by a) creating envelopes of the experimental reverse-cyclic responses; b) the proposed analysis method; and c) analysis that assumed the walls to respond only by rocking. The figure shows that accounting for all three response mechanisms improves correlation between the total posttensioning forces and the experimentally measured responses. This is because the increase in posttensioning force due to wall in-plane displacements is mainly dependent on $\Delta_{rocking}$. When all three mechanisms are included in the analysis, $\Delta_{rocking} < \Delta_{total}$, which leads to lower posttensioning forces than analysis that assumes only the rocking response, where $\Delta_{rocking} = \Delta_{total}$. Despite the improvements, the presented analysis method is still unable to provide very accurate estimates for the posttensioning forces. As discussed previously, this behavior is due, in part, to the monotonic analyses not including any effects from the reverse-cyclic wall responses. It has been confirmed that including these effects can improve accuracy of the analyses significantly [15].
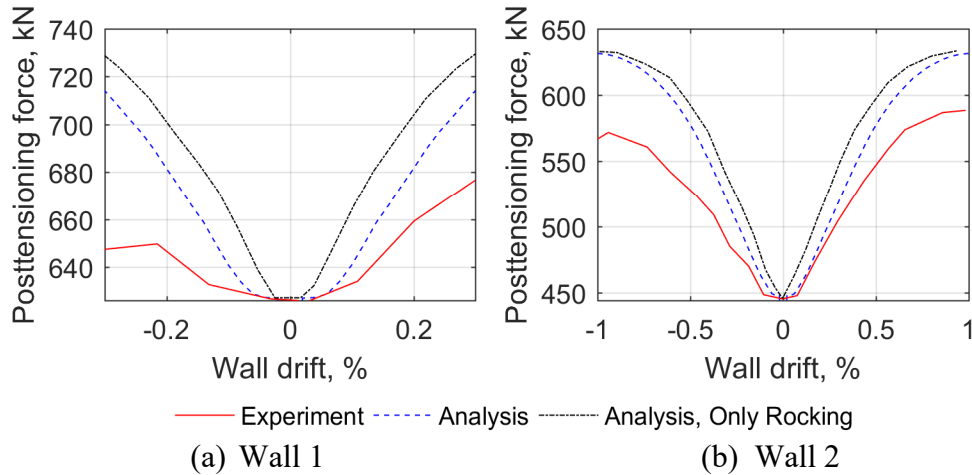
(a) Wall 1   (b) Wall 2

Figure 3: Posttensioning force vs. wall top in-plane drift

Finally, Figure 4 compares the total in-plane displacements with the displacements due to rocking rotation, flexure, and shear as they are estimated a) by the proposed analysis method; and b) from the experiments [12]. Both the presented analysis method and experiments confirm that the rocking responses dominate the overall wall responses. For example, at wall drift of 0.5%, both analysis and experiment indicate the wall drift due to rocking to be 87% of the total wall drift for Wall 1. The rocking response is shown to reduce for Wall 2 due to its increased slenderness: at the wall drift of 0.5%, analysis and experiment indicate the drift due to rocking to be 82% of the total wall drift. Overall, the figure shows that the analysis method adequately captures the amount of rocking, flexure, and shear responses as estimated from the experimental measurements, for both walls. It also confirms that accurate estimation of wall displacements must include the flexure and shear components. Otherwise, errors on the order of 13 and 18% in the computed displacements of the walls may be present in analyses that account only for the rocking mechanism.
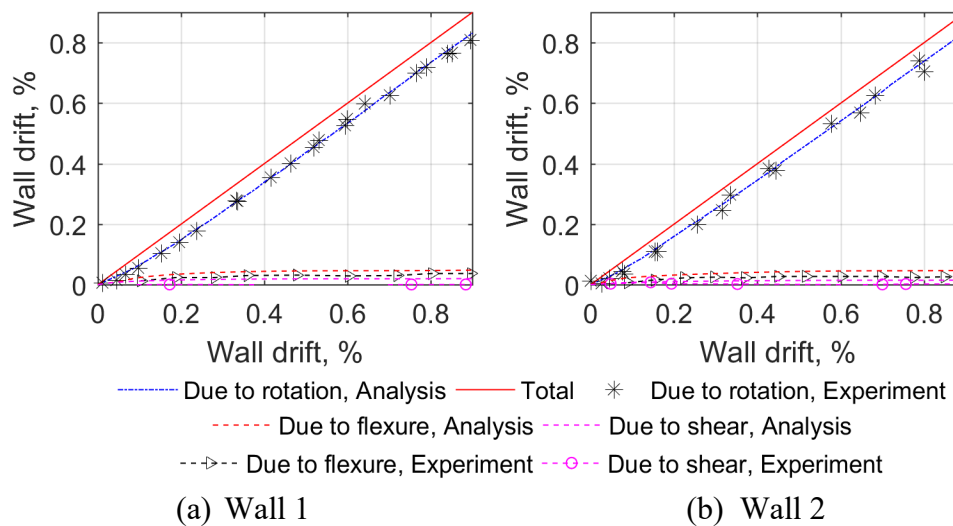

(a) Wall 1   (b) Wall 2

Figure 4: Total wall drift vs. wall drift only due to rocking

CONCLUSIONS

Previous envelope analysis approaches for masonry walls designed with unbonded-posttensioning characterize their behavior assuming a rocking response with limited consideration to other response mechanisms, which is inconsistent with experimental observations. To address this concern, this paper has introduced an analysis method that includes the flexure and shear responses of these masonry walls in addition to rocking.

Similar to the experiments, the proposed analysis method predicted rocking to dominate the wall responses. For the walls considered in this paper, the displacements due to flexure and shear were analytically found to contribute up to 18% of the total wall displacements, for a wall drift of 0.5%.

The proposed analysis method slightly improved estimation of the posttensioning forces due to wall in-plane displacements compared to analyses that assumed only rocking response. Even though there was an improvement, the use of a monotonic analysis method was found to not accurately capture the increase in posttensioning forces. This was attributed to the monotonic analysis being unable to reproduce the response characteristics associated with the reverse-cyclic displacement-histories of the walls, as they were used in the experiments.

Overall, the proposed analysis method was found to more accurately estimate the wall responses by accounting for all three mechanisms of flexure, shear, and rocking.

REFERENCES

[1] Housner, G. W. (1963). "The behaviour of inverted pendulum structures during earthquakes." *Bulletin of the Seismology Society of America*, 53, 404-417.

[2] Priestley, M J. N. Sritharan, S. Conley, J. R. and Pampanin, S. (1999). "Preliminary results and conclusions from the PRESSS five-story precast concrete test building." *PCI Journal*, 44(6), 42-67.

[3] Schultz, A. E. and Magana, R. A. (1998). "Performance of precast concrete shear walls." *6th U. S. National Conference on Earthquake Engineering*, Earthquake Engineering Research Institute.

[4] Sritharan, S. Aaleti, S. Henry, R. H. Liu, K. Y. and Tsai, K. C. (2015). "Precast concrete wall with end columns (PreWEC) for earthquake resistant design." *Earthquake Engineering and Structural Dynamics*, 44(12), 2075-2092.

[5] Kalliontzis, D. and Sritharan, S. (2014). "A finite element approach for modelling controlled rocking systems." *2nd European Conference on Earthquake Engineering Seismology*, A joint event of 15th European Conference on Earthquake Engineering & 34th General Assembly of the European Seismological Commission, Istanbul, Turkey, 25-29 Aug.

[6] Kalliontzis, D. Sritharan, S. and Schultz, A. E. (2016). "Improved coefficient of restitution estimation for free rocking members." *Journal of Structural Engineering*, ASCE, 10.1061/(ASCE)ST.1943-541X.0001598,06016002.

[7] Kalliontzis, D. and Sritharan, S. (2016). "A simple analytical model for the rocking PreWEC system." *VII European Congress on Computational Methods in Applied Sciences and Engineering* (ECCOMAS), Crete Island, Greece.

[8]   Nazari, M. Sritharan, S. and Aaleti, S. (2016). "Single precast concrete rocking walls as earthquake force-resisting elements." *Earthquake Engineering and Structural Dynamics*, DOI: 10.1002/eqe.2829.

[9]   Laursen, P. T. and Ingham, J. M. (2001). "Structural testing of single-storey posttensioned concrete masonry walls." *TMS Journal*, September, 69-82.

[10] Rosenboom, O. A. and Kowalsky, M. J. (2004). "Reversed in-plane cyclic behavior of posttensioned clay brick masonry walls." *Journal of Structural Engineerin*g, ASCE, 10.1061/(ASCE)0733-9445(2004)130:5(787), 787-798.

[11] Hassanli, R. ElGawady, A. and Mills, J. E. (2016). "Experimental investigation of in-plane cyclic response of unbonded-posttensioned masonry walls." *Journal of Structural Engineering*, ASCE, 142(5), 04015171.

[12] Laursen, P. T. and Ingham, J. M. (2000). "Cyclic in-plane structural testing of prestressed concrete masonry walls." *Phase 1: Simple Wall Configurations, Volume A: Evaluation of Wall Structural Performance*, Department of Civil and Environmental Engineering, University of Auckland, Auckland, New Zealand.

[13] Huizer, A. and Shrive N. (1986). "Performance of a post-tensioned single wythe clay brick masonry wall subjected to shear." *Proc. 4th Canadian Masonry Symposium*, 612-621.

[14] Kalliontzis, D. and Schultz, A. E. (2017). "Characterizing the in-plane rocking response of masonry walls with unbonded post-tensioning." *Journal of Structural Engineering*, ASCE (in press).

[15] Kalliontzis, D. and Schultz, A. E. (2017). "Improved estimation of the reverse-cyclic behavior of fully-grouted masonry shear walls with unbonded post-tensioning." *Engineering Structures* (under review).

[16] MSJC (Masonry Standards Joint Committee). (2013). "Building code requirements for masonry structures." *ACI 530/ASCE 5, TMS 402*, American Concrete Institute, Detroit.

[17] Priestley, M. J. N. and Elder, D. M. (1983). "Stress-strain curves for unconfined and confined concrete masonry." *ACI Structural Journal*, 80(3), 192-201.